Ocean biomass-derived feedstocks for non-isocyanate polyurethane synthesis†

Jane E. Peddle, Courtney M. Laprise, Mikhailey D. Wheeler, [iD] Megan M. Fitzgerald, Francesca M. Kerton [iD] and Christopher M. Kozak [iD] *

Non-isocyanate polyurethanes (NIPUs) can be prepared from the highly unsaturated oils or fatty acid methyl esters obtained from waste fish and algae oil. The abundant carbon–carbon double bonds can be epoxidized and reacted with CO_2 to produce cyclic carbonates. Upon reaction with a bioderived amine from waste cashew nutshells, a NIPU is obtained. Fish-oil derived NIPUs were studied for biodegradation and were found to be susceptible to degradation by bacteria and fungi. Algae oil tri- and diacylglycerides were converted to their fatty acid methyl esters (FAMEs) and used for the preparation of NIPUs in a similar fashion to fish oil. NIPUs could be obtained as thermoset films, which were characterized *via* infrared spectroscopy to verify urethane linkage formation and dynamic mechanical analysis for their physical properties. These processes can lead to new opportunities in waste valorization of the aquaculture industry and demonstrate the promise of algae as an abundant source of biomass.

Introduction

Bio-based polyurethanes (PUs) have attracted considerable attention recently as ecologically-sustainable alternatives to their traditionally petroleum-derived materials.[1–4] Biodegradable plastics from renewable feedstocks have been proposed as replacements for the petrochemical materials, however, there are few monomers available that can be directly substituted for those in current use.[5]

Traditional PUs are produced by step-growth copolymerization of polyols and diisocyanates, produced from reacting amine compounds with toxic phosgene. Isocyanates are also moisture sensitive, making stable storage problematic.[6] As a result, non-isocyanate routes to PU synthesis have become increasingly important.[7–10] The reaction of 5-membered cyclic carbonates with amines is among the more promising routes to the synthesis of non-isocyanate polyurethanes (NIPUs). The cyclic carbonates are obtained *via* a catalyzed coupling reaction of CO_2

Department of Chemistry, Memorial University of Newfoundland, St. John's, Newfoundland, A1C 5S7, Canada. E-mail: ckozak@mun.ca

with epoxides. The resulting carbonates are typically robust and provide an approach that contributes to potential CO_2 sequestration. The aminolysis step performs a ring-opening of the carbonate group, forming a hydroxyl group adjacent to the urethane linkage, thereby producing a poly(hydroxyurethane) (PHU).

The epoxide-containing reactant can be prepared *via* numerous epoxidation reactions on unsaturated (olefinic) substrates. Where the variety of suitable olefinic substrates is vast, this permits enormous potential for variability in both structure of the epoxide (and the cyclic carbonate it produces) and its source, for example, biomass-derived unsaturated oils and fatty acids. The most common bioderived oils used to prepare carbonates for use in NIPU synthesis are soybean or linseed oil, which contain many mono- and poly-unsaturated fatty acids.[11–15] Soybean oil, which is perhaps the most widely used bioderived oil for NIPU synthesis, utilizes a large amount of land space, reducing the amount of land available for other food producing crops. A potential alternative to plant-based oils are oils derived from aquaculture waste or non-food plant sources, such as microalgae and macroalgae (seaweeds). Algae is a particularly promising feedstock for many applications including biofuels as well as polymeric materials because of its high oil content.[16–18] Algae produce polyunsaturated fatty acids (PUFAs), such as eicosapentaenoic acid (EPA, C22:5) and docosahexaenoic acid (DHA, C22:6), which make good candidates for generating highly cross-linked NIPUs.[19] We have previously reported the use of waste fish oil as a source of olefin-rich material for epoxidation and cyclic carbonate formation. The fish-oil carbonates were cross-linked through aminolysis with Cardolite™ phenalkamine NC-540,[20] a triamine derived from cardanol, a phenolic lipid obtained from cashew nutshells, to give NIPUs.[21] In this study, we describe degradation studies of fish oil-derived NIPUs and the preparation of NIPUs using algae oil as a source of polyunsaturated fatty acids and NC-540 as a curing agent.

Results and discussion

General compositions of fish oil and algae oil glycerides

The major fatty acids in fish oil (FO) are oleic (C18:1ω-9, 31%), linoleic (C18:2ω-6, 15%), palmitic (C16:0, 14%), and palmitoleic (C16:1ω-1, 7%) acid.[22] The major fatty acid components of algae oil are monounsaturated fatty acids (37.0%) including palmitoleic and oleic acids, polyunsaturated fatty acids (16.2%) including eicosapentaenoic acid (C20:5) and docosahexaenoic acid (C22:6) and saturated fatty acids (35.0%) including palmitic and myristic (C14:0) acids.[19,23] In our previous work with FO, the triglycerides were used for epoxidation, carbonation and curing with Cardolite™ NC-540[20] to give NIPU products (Scheme 1).[21] NIPU preparation from carbonated algae oils has been reported previously using diamines, such as butane diamine, pentane diamine and octane diamine as cross-linkers,[19] but the use of NC-540 with algae-oil derived carbonates is novel. Where NC-540 is a triamine containing primary and secondary amines with a phenol group, linkages may be formed through any or all of these functionalities. At present we cannot distinguish linkages formed from the primary or secondary amines, or the phenol. Unlike traditional plant oils,[24,25] in addition to triglycerides, algae possess diacylglycerides with galactosyl or phosphate groups on the third hydroxy functionality of glycerol.[26] This results in difficulty in extraction of fatty acids using hydrocarbon solvents due to the presence of polar
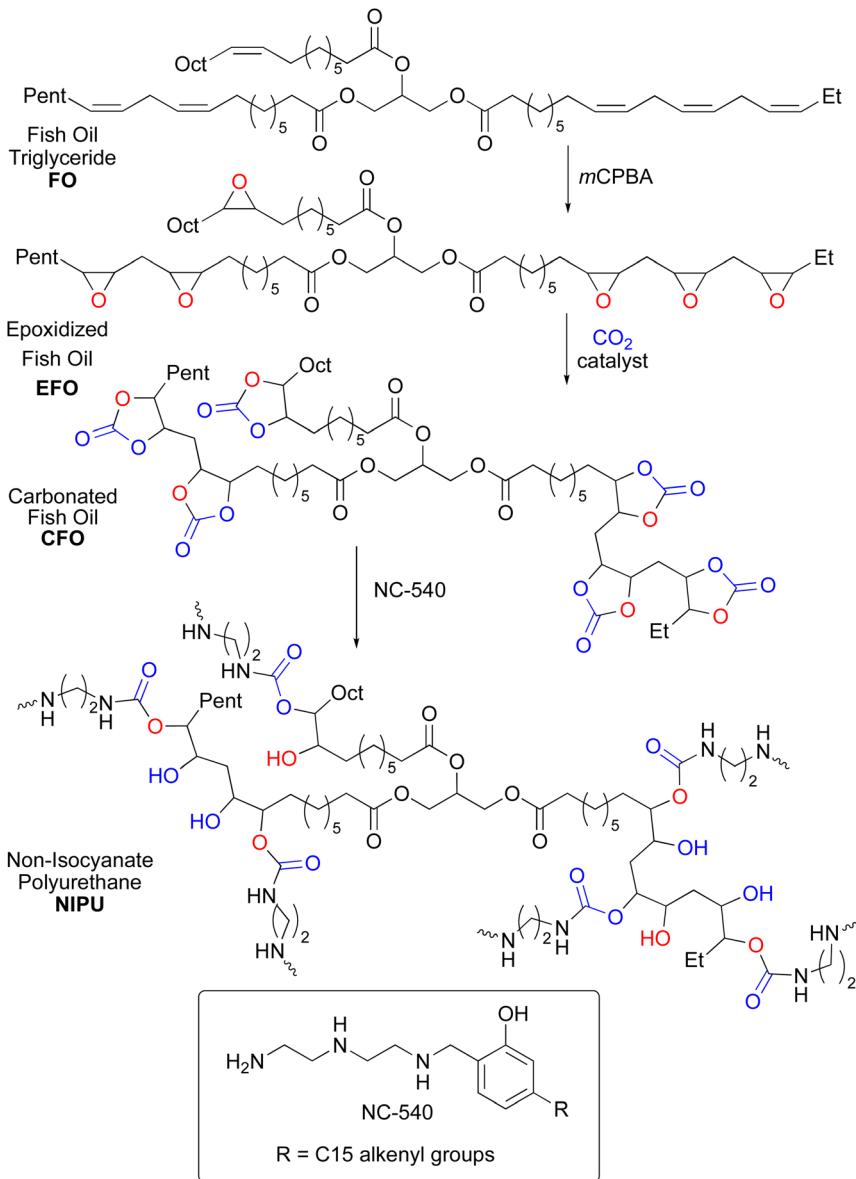
Scheme 1 Synthesis of carbonated fish oil triglyceride (CFO) and preparation of FO-based NIPU from CFO and Cardolite™ NC-540.

substituents on the glyceride.[23] For this work, the algae oil (AO) was converted to FAMEs and the isolated esters were used for epoxidation and subsequent study, whereas fish oil could be used directly without conversion to FAMEs.

Behaviour of fish oil-derived non-isocyanate polyurethane materials in water and enzymatic degradation studies

Behaviour of films in fresh and saltwater aqueous environments. To study the degradability of the previously reported FO-NIPU material[21] in aqueous solutions,

pieces of the film were stirred in deionized water, synthetic sea water, and sea water collected from Middle Cove Beach, NL, Canada. Cuts of the translucent red NIPU film (Fig. 1A) were placed in an Erlenmeyer flask, each with 100 mL of the appropriate aqueous solution, sealed and shaken at 290 rpm. The synthetic sea water used was made to a concentration of 33 g L^{-1}, the global average salinity of sea water, with sea salts. The resulting synthetic sea water had the approximate concentration of ions presented in Table 1. After 28 days of stirring, the NIPU films were removed from the aqueous solutions, resulting in the films shown in Fig. 1. Changes in the masses of the films are shown in Table 2 below. The film in deionized water was light orange and opaque (Fig. 1B), and its mass after stirring was 187% its original mass, indicating that there was a large uptake of deionized water. After leaving the film to dry overnight in the open air, the film lost a large portion of this water and was 120% its original mass. When replicate experiments were performed, similar weight percent changes were observed regardless of the original mass of NIPU film. After stirring for 28 days in synthetic sea water the film retained the red colour but became opaque (Fig. 1C). Its mass swelled to 112% of its original mass and after drying in air overnight the film returned to its original mass. The film that was exposed to real sea water collected from Middle Cove Beach, NL, Canada, also remained reddish-orange and became opaque. The weight changes seen with the film were like those of the synthetic sea water film, with its mass being 120% its original mass after stirring and losing all the absorbed water after drying in air overnight.

The surfaces of the NIPU films were analyzed by scanning electron microscopy (SEM). The original film (Fig. 2A and B) shows an undulating surface with no visible perforations. The film shaken in deionized water (Fig. 2C and D) shows the presence of small perforations, potentially caused by its swelling from absorption of water and its release upon drying. The film shaken in synthetic sea water
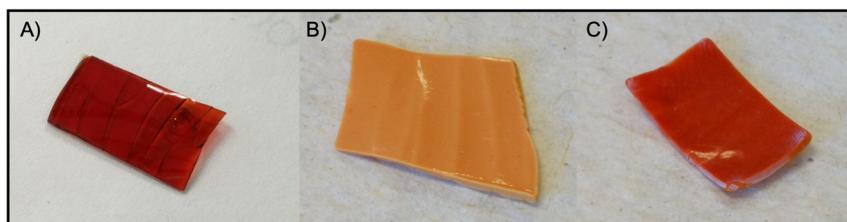

Fig. 1 FO-NIPU films (A) and after 28 days in deionized water (B) and sea water (C).

Table 1 Ion concentrations in synthetic sea water for aqueous degradation studies

Ion	Concentration (mg L^{-1})
Chloride	17 000
Sodium	9500
Magnesium	1100
Potassium	350
Calcium	350
Carbonate	170

Table 2 FO-NIPU masses before and after exposure to water or sea water for 28 days

| Entry	Medium	Starting mass (mg)	Weight after stirring (%)	Weight after drying (%)
1	Deionized water	31.0	187	120
2		10.6	168	112
3	Synthetic sea water	31.6	112	100
4		37.0	123	103
5	Sea water, MC[a]	28.7	120	102

[a] MC = Middle Cove Beach, NL.
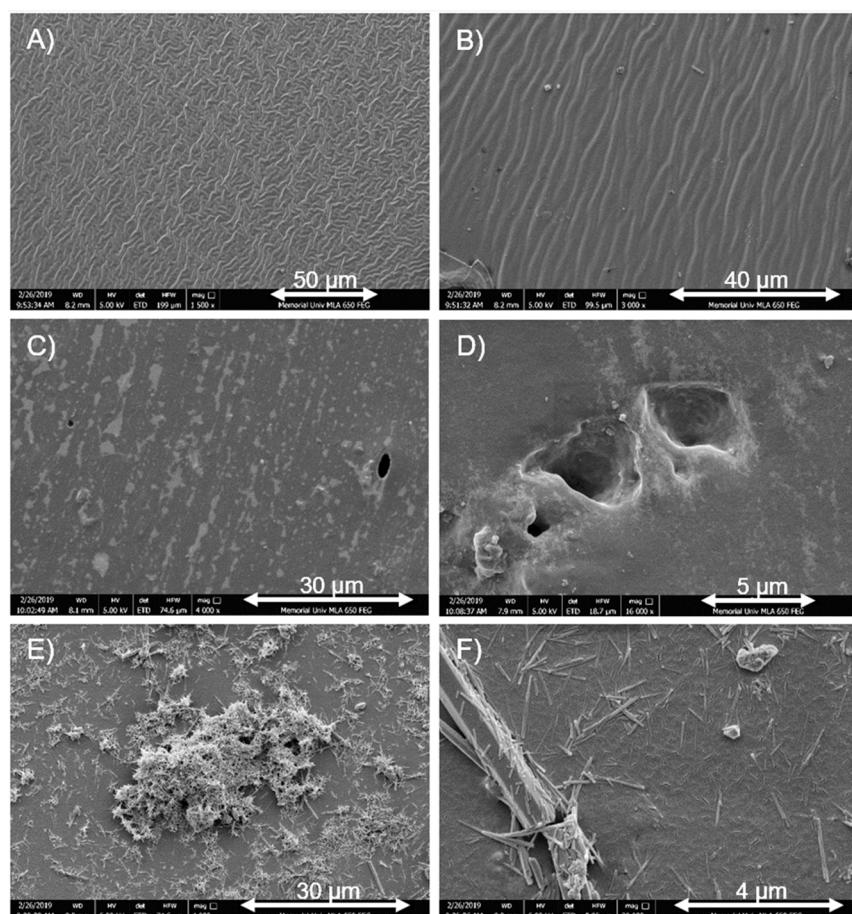
Fig. 2 Selected, typical SEM images of FO-NIPU films exposed to water for 28 days, (A and B) original film, (C and D) deionized water NIPU film, and (E and F) synthetic sea water NIPU film.

(Fig. 2E and F) shows long needle-like salt crystals throughout the surface of the film, which show some embedding into the surface. These crystals appear in large agglomerations regularly over the surface of the film. Duplicate samples showed identical behaviour under SEM.

SEM energy dispersive X-ray (SEM-EDX) spectroscopy determined the elemental composition of the crystals on the surface of the film exposed to synthetic sea water. An EDX spectrum (Fig. 3) of the crystalline deposits shows the presence of calcium, oxygen, potassium, chlorine, sodium, and magnesium. These are expected given the ion concentrations present in the synthetic sea water (Table 1). Elemental maps of the elements of interest were generated for the same agglomerations of crystals (Fig. 4). Sodium and chlorine are present on the surface of the film but not specifically localized to the crystals. Large amounts of calcium and oxygen are found localized within the crystals, likely calcium carbonate ($CaCO_3$). Magnesium appears to be present in regions corresponding to larger crystals on the surface of the film, which may correspond to either $MgCO_3$ or mixed group 2 carbonates ($Mg_xCa_yCO_3$).

SEM and elemental mapping of the FO-NIPU film after exposure to real sea water was also performed (Fig. 5). This film is also covered with needle-like crystals but with a different composition to those obtained from synthetic sea water exposure. The elemental maps show the presence of mostly sodium and chlorine, with some magnesium throughout. There is a much lower presence of calcium and oxygen, mostly found in particles around the regions where sodium and chlorine are found. The material is therefore likely NaCl with small amounts of $MgCl_2$ and $CaCO_3$. The difference in salt composition on the surfaces of the films is due to differences in salinity of the solutions. The synthetic sea water was
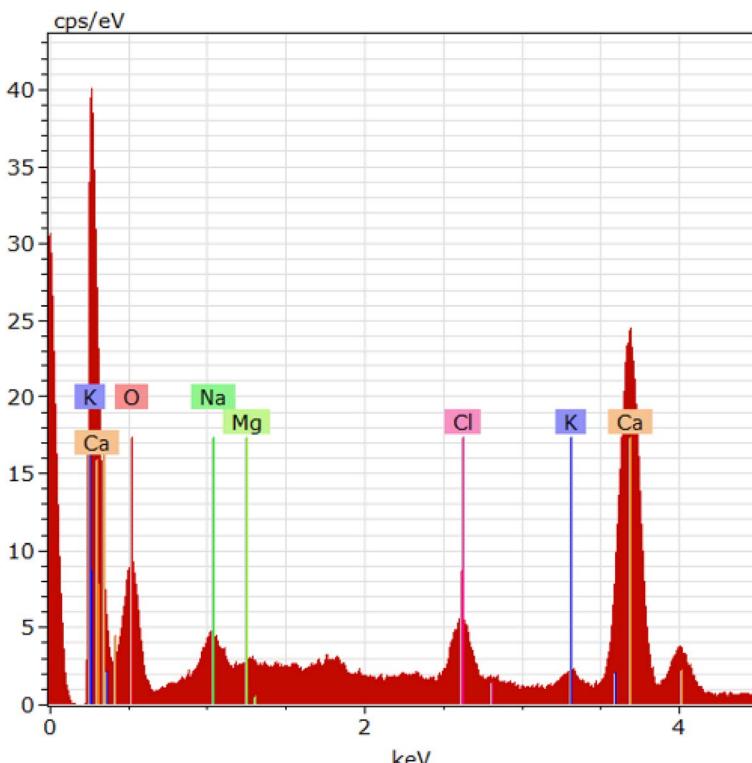

Fig. 3 EDX spectrum of crystals on film exposed to synthetic sea water.
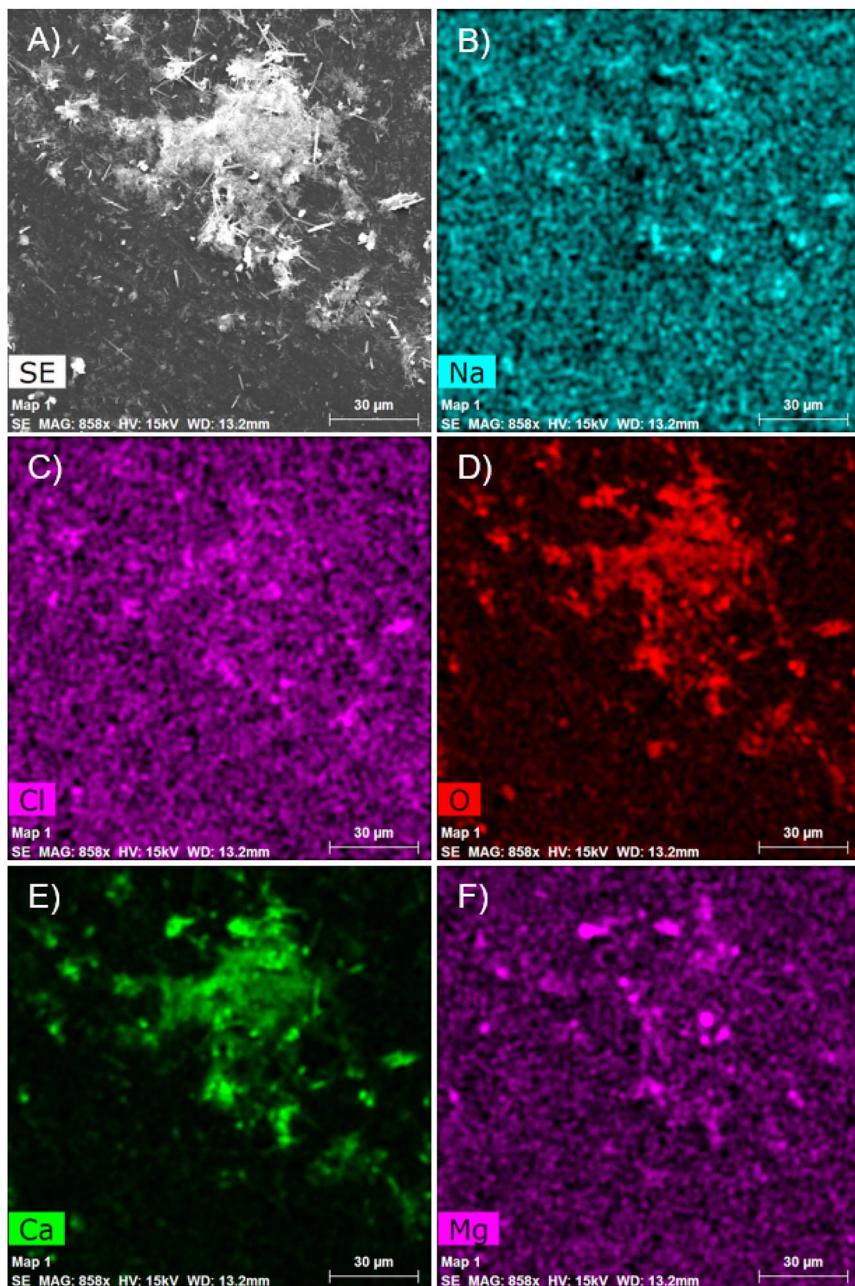
Fig. 4 SEM-EDX elemental maps of crystalline material found on the surface of the FO-NIPU film after exposure to synthetic sea water. (A) SEM image of agglomerate and elemental maps of (B) sodium, (C) chlorine, (D) oxygen, (E) calcium, and (F) magnesium.

prepared to the global average salt concentration in sea water, whereas the sea water collected from Middle Cove Beach has a much lower salinity than the global average, due to several fresh-water streams flowing into the cove. Real sea water contains microorganisms that are not present in the synthetic sea water, which
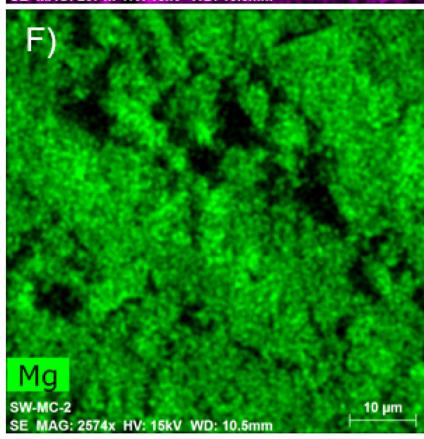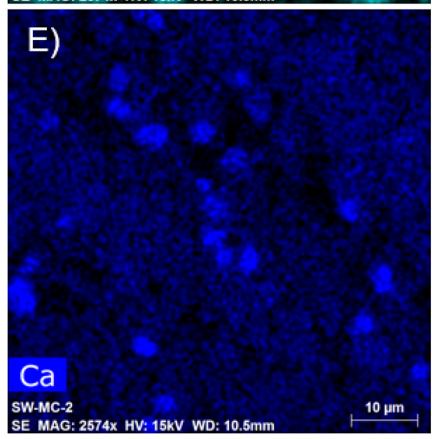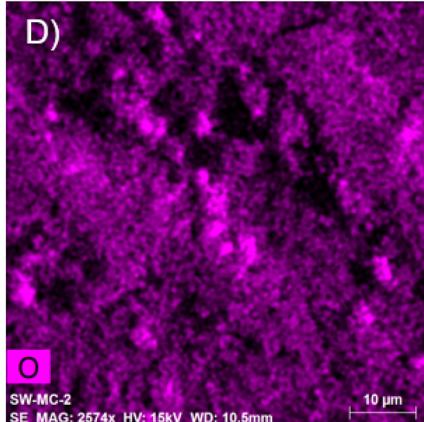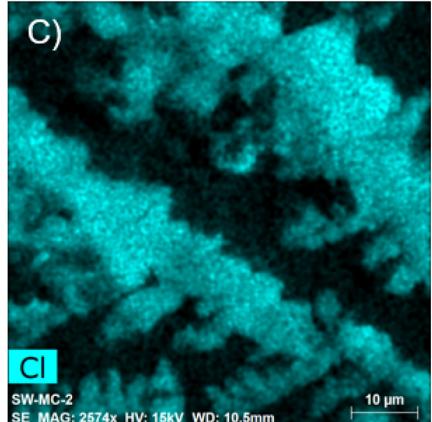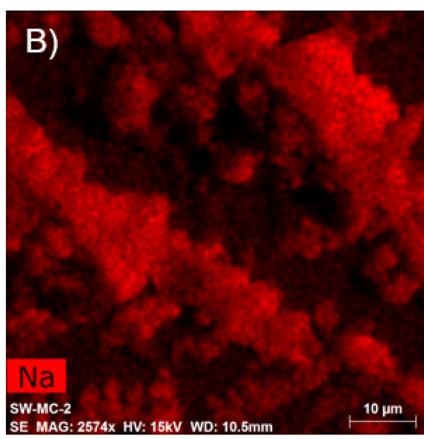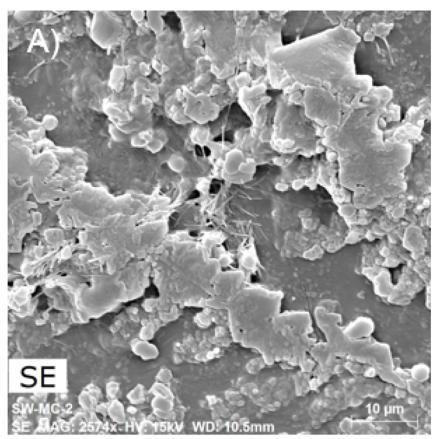
Fig. 5   SEM image of the surface of FO-NIPU film exposed to Middle Cove sea water (A), and elemental maps of (B) sodium, (C) chlorine, (D) oxygen, (E) calcium, and (F) magnesium.

was produced using sterile deionized water. As a result, mostly $CaCO_3$ forms on the FO-NIPU surface exposed to synthetic sea water, but NaCl forms when exposed to real sea water.

IR spectroscopy was used to compare the original FO-NIPU material before and after stirring in deionized water and sea water (Fig. 6). The film shaken in deionized water shows an increase in the –OH region around 3290 cm^{-1} due to the large amount of water present in the film even after drying. In the spectrum of the film exposed to sea water, additional bands are observed around 1460 cm^{-1} and at 874 cm^{-1}. The band at 1460 cm^{-1} is typical of amorphous $CaCO_3$, while the sharp band at 874 cm^{-1} suggests a calcite phase.[27] This agrees with the EDX spectrum and the elemental maps, indicating that $CaCO_3$ is present on the surface of the sea water film.

Both films exposed to real and synthetic sea water showed a decreased uptake of water compared to films that were shaken in deionized water. While the film exposed to real sea water had mostly NaCl on its surface, the film exposed to synthetic sea water had predominantly $CaCO_3$ on its surface. An SEM image of the film shaken in synthetic sea water, taken after 30 min of stirring (Fig. 7), shows formation of crystals on the surface of the film. This early crystal growth potentially inhibits the uptake of water by the film, causing films to absorb less water in either type of saltwater used, and this means that the films show little deformation or degradation when compared to the film shaken in deionized water that contained holes. This may ultimately impact the ability for these FO-NIPU films to undergo degradation in ocean environments as the salinity may lead to encrusting of the surface, limiting penetration of water into the film.

Enzymatic degradation studies. To study the enzymatic degradability of the FO-NIPU, a method similar to that previously reported for the investigation of enzymatic hydrolysis of polyester elastomers was used,[28] but using a lipase enzyme rather than a cutinase. 5 mm × 5 mm squares of the film were placed in buffered solutions containing Novozym® 51032 lipase enzyme. After 14 days in
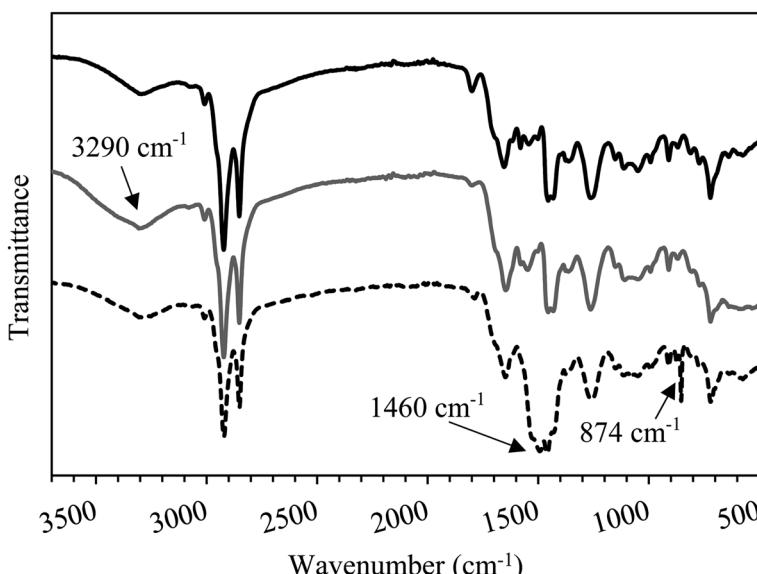

Fig. 6 IR spectra of FO-NIPU (black, top), deionized water NIPU (gray, middle), and sea water-exposed FO-NIPU (black dashed, bottom).
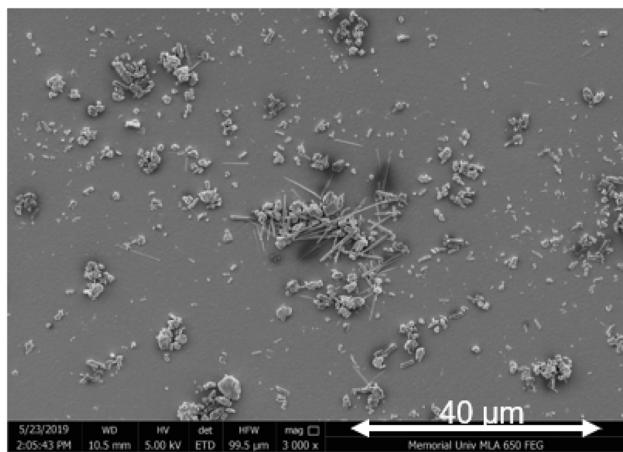
Fig. 7   SEM image of synthetic sea water FO-NIPU film after 30 min.

the enzyme solution, the film had curled with microbial growth appearing on the inner side of the film and within the solution. After 22 days, one sample was removed from its solution and characterized. The film turned light beige in colour and remained curled up (Fig. 8A). A brownish-green mold covered the inner surface of the film (Fig. 8B), while the outside remained shiny and smooth. The
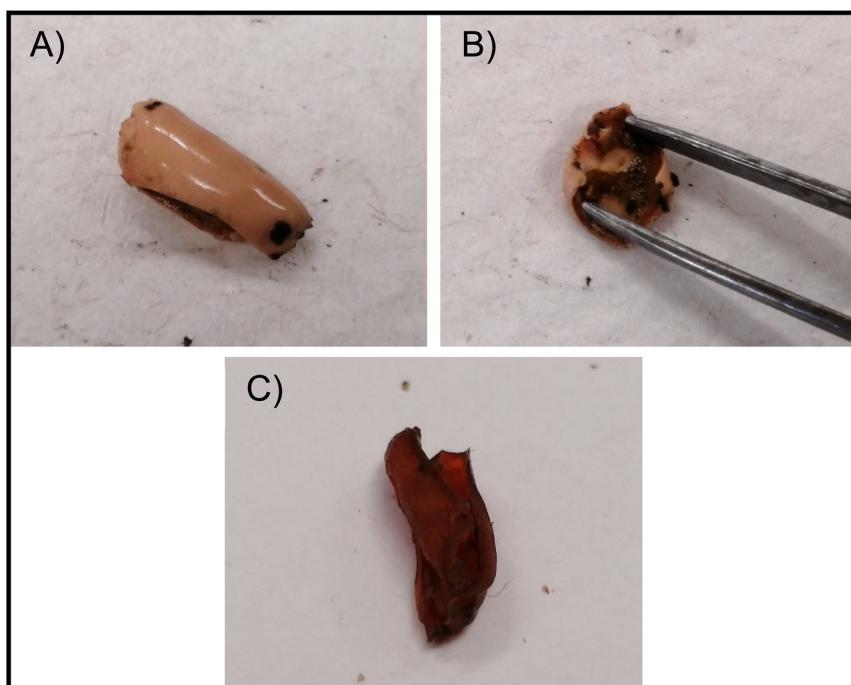

Fig. 8   Images of degraded NIPU film. (A) and (B) show film after removal from solution and (C) after drying in air overnight.

mass of the film had increased by 2.8× its original mass. After drying in the open air overnight the film returned to a dark red colour but had become hard and brittle (Fig. 8C).

SEM was performed on the film samples obtained from soaking in the enzymatic solution. The surface of the film displayed cracks and fissures suggesting degradation (Fig. 9A and B), with thread-like masses present (Fig. 9C), which are potentially the hyphae from a mold. Small, clustered particles were also found that could be the bacteria and its produced spores (Fig. 9D). Microbial growth can be prevented by addition of sodium azide to solutions used in enzymatic degradation studies,[29] but we were intrigued to find out which microbes would grow under such conditions. Microbes that grew on the FO-NIPU films were identified as *Exophiala* and *Gloeotinia* fungi, and *Paraburkholderia* bacteria. These fungi and bacteria have also been observed during decomposition studies of polycaprolactone/biochar composite materials.[30] The hypothesized species of fungi are *Exophiala oligosperma* and *Simplicillium chinense* or *Leptobacillium leptobactrum*. The genus *Paraburkholderia* comprises a wide variety of environmental bacteria that are found associated with plant and fungal tissues, and the two hypothesized species that grew on the FO-NIPU film are *P. madseniana* or *P. fungorum*.[31] *P. madseniana* are recently discovered bacteria and show excellent performance at breaking down organic matter raising speculation about its role in carbon cycling,[32] whereas *P. fungorum* have been used to improve growth, yields, and contents of antioxidants in plants.[33] The fungi *E. oligosperma* and *S. chinense* are usually isolated from environmental sources such as soil or water.[34,35] These preliminary degradation results suggest that these NIPU materials can support growth of microbes that are present in the environment. The exact
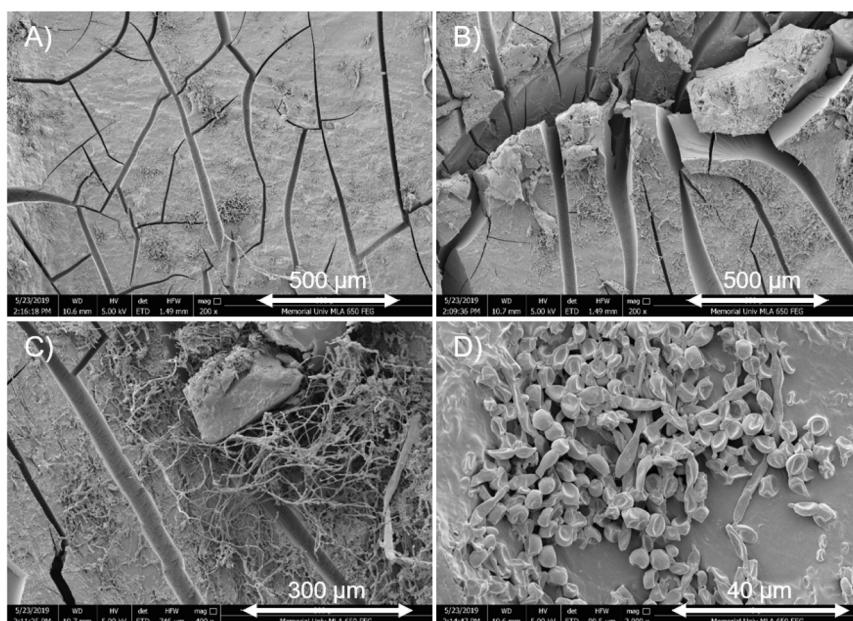

Fig. 9 SEM images of degraded NIPU film. (A) and (B) surface of film, (C) mold hyphae, and (D) clusters of bacteria on surface.

microbes present are dependent upon specific geographic location and climate, therefore, further studies in other locations are needed to assess degradation potential.

Synthesis of NIPU from algae oil-derived fatty acid methyl esters

Characterization of algae oil. Oil was obtained from the microalgae *Schizochytrium* sp., which is a heterotrophic microalgae that can yield about 40% (w/w) of docosahexaenoic acid (DHA) from its total fatty acid production.[36] As mentioned above, algae oil contains a mixture of triglycerides and diacylglycerides with galactosyl or phosphate groups, therefore, the oil was transesterified in alkaline methanol to yield fatty acid methyl esters (FAMEs), which were then used for NIPU production. The algae oil was characterized by ^{1}H and ^{13}C NMR spectroscopy and FTIR spectroscopy (see ESI†). Algae oil was found to be stable under long term storage at 3 °C as shown by NMR spectra taken 1 year apart. The ^{1}H NMR spectrum shows the expected resonances corresponding to methyl and methylene groups of saturated components of the fatty acid chains, while peaks from δ 2.02–2.12 correspond to methylene protons adjacent to double bonds. Resonances at δ 2.28–2.38 correspond to methylene protons adjacent to the ester carbonyl groups. The glycerol backbone gives resonances at δ 4.11–4.33 with multiplets at δ 5.36–5.39 corresponding to the olefinic protons. FTIR spectroscopy shows bands at 2853 to 3012 cm^{-1} corresponding to alkene and alkane C–H stretches. The ester carbonyl band is observed at 1743 cm^{-1} and those observed at 1146 cm^{-1} and 1098 cm^{-1} correspond to the stretching mode of C–O bonds.

Transformation of the algae oil to its FAMEs was conducted through transesterification in alkaline methanol giving 82% isolated yields. The purified FAMEs are less viscous than the algae oil facilitating their epoxidation and carbonation reactions. The FAMEs were analyzed using ^{1}H and ^{13}C NMR spectroscopy, FT-IR spectroscopy, and GC-MS (ESI). The ^{13}C NMR spectrum for the FAMEs shows the presence of two carbon resonances at δ 51.4 and 51.6 attributed to CH_3–O–(C=O) groups,[37] indicating multiple fatty acid chains. The IR spectrum of the FAME showed a slight decrease in the intensity of the band corresponding to the stretching mode of a C–O bond but otherwise was very similar to the IR spectrum of the algae oil. The FAME mixture was analyzed by GC-MS and showed the presence of multiple fatty acid chains consistent with those reported by others.[38]

Table 3 DMA data for NIPU collected in duplicate

Sample	1	2	Average
Stress at break (MPa)	0.18	0.08	0.13
Strain at break (%)	52.37	43.68	48.03
Initial length (mm)	5.44	5.55	5.50
Length at break (mm)	8.51	7.73	8.12
Elongation at break (%)	56.4	39.2	47.8
E (kPa)	5.11	3.73	4.42
Width (mm)	5.68	6.11	5.90
Thickness (mm)	0.70	0.82	0.76
Young's modulus (Pa)	5.1	3.7	4.4

Epoxidation of algae oil FAMEs. Epoxidation of the FAMEs was performed using *m*-CPBA. We previously reported other epoxidation routes including acid catalyzed epoxidation using H_2O_2 but *m*-CPBA consistently gave higher yields of epoxides in shorter times.[21] The percent conversion of C=C double bonds to epoxy groups was determined by ^{1}H NMR spectroscopy (ESI†). As we have previously observed for epoxidation of fish oil,[21] and others have observed for epoxidation of algae oil, epoxidation of the double bonds was found to be quantitative.[19] Infrared spectroscopy of the epoxidized FAMEs (EFAMEs) showed the clear loss of alkene =C–H stretches at 3013 cm^{-1} but other stretches attributable to alkenes below 1700 cm^{-1} or their disappearance upon epoxide formation could not be confirmed (ESI†).

Carbonation of epoxidized FAMEs. Epoxidized FAMEs were reacted with CO_2 (10 bar) in the presence of catalytic amounts of tetrabutylammonium bromide (TBAB) and ascorbic acid following our previously reported procedure.[21] The percent conversion from the epoxide to the cyclic carbonate was determined by ^{1}H NMR spectroscopy to reach up to 80%. Characteristic peaks for the formation of the cyclic carbonate typically appear at δ 4.2 and 4.6 (see ESI†).[39] IR spectroscopy showed evidence of cyclic carbonate formation with the appearance of a new carbonyl band at 1791 cm^{-1} in agreement with those observed for carbonated plant-derived oils.[13,14,40,41]

Polymer formation

Carbonated FAMEs were used for NIPU production through cross-linking with Cardolite™ NC-540 curing agent. NC-540 is a mixture of phenalkamines prepared from cardanol, which is derived from waste cashew nut shells (Scheme 1). It is made *via* a modified Mannich reaction with formaldehyde and a triamine and has been used as a curing agent to produce a range of materials.[41] With a desire to prepare a fully biobased NIPU, we performed reactions with this commercially available amine mixture. The algae oil FAME-based NIPU was obtained by mixing NC-540 in a ratio of 2 : 1 by mass with the CFAME on a glass Petri dish and heating to 40 °C. This was then placed uncovered in an oven at 100 °C for 24 h to cure. The resulting thermoset polymer was characterized upon cooling. The 2 : 1 ratio of NC-540 to CFAME was chosen based on conditions we previously reported for fish oil carbonates,[21] and this ratio produced films of suitable thickness and durability for dynamic mechanical analysis (DMA) measurements.

As expected, the flexible, red, transparent NIPU films obtained were found to be insoluble in common deuterated solvents (chloroform, acetone, benzene); therefore, analysis by NMR was not performed. Infrared spectroscopy on the NIPU material confirmed the formation of urethane linkages. Compared to the carbonated FAME, there is a weakening of the carbonate band at 1735 cm^{-1} and new bands at 1665 cm^{-1} and 3305 cm^{-1}, which are characteristic of N–H bends and O–H/N–H stretches, respectively.

DMA measurements were performed on the produced NIPU materials. As the curing of the NIPU was performed crudely, the materials obtained did not possess uniform thickness leading to variability in the measurements of the Young's modulus and elongation at break. The DMA results for polyurethanes obtained from curing EFAMEs with NC-540 gave elongations at break of 47.8 ± 8.6% and a Young's modulus of 4.4 ± 0.7 Pa. A representative stress *vs.* strain plot is given in the ESI.†

Conclusions

Our latest investigations into the utility of ocean-derived fish and algae biomass as a feedstock for synthesis of polymers are described. Preliminary results show fish oil-derived NIPUs are susceptible to microbial degradation. Further studies are needed to quantify the extent of degradation. Algae oil can also be used as a feedstock for unsaturated monomers and can be converted to FAMEs. These can be epoxidized rapidly using *m*-CPBA and converted to cyclic carbonates *via* catalytic CO_2 cycloaddition under moderate pressure. In a similar way to fish oil-derived carbonates, these carbonates can be cured with a cardanol-derived phenalkamine cross-linker, NC-540, to give mildly elastic thermoset films. Further analysis is required to determine thermal properties of the material and the effects of varying the ratio of carbonate to cross-linker, and biodegradation studies on algae-derived materials.

Experimental

Materials

Algae oil obtained from *Schizochytrium* sp. was purchased from Jedwards International Inc. (product number 002261065). Solvents were purchased from Fisher Scientific. 3-Chloroperbenzoic acid (*m*-CPBA) (≤77%) was purchased from Sigma Aldrich. Cardolite™ (NC-540) (≤9.0% 2,2′-iminodiethylamine) was provided from Cardolite Corporation. All reagents were used as received from the supplier without further purification. Synthetic sea water, 35 parts per thousand (ppt) or 35 g L^{-1}, was prepared using sea salts purchased from Sigma Aldrich. Natural sea water was collected from Middle Cove Beach, NL (47°39′2.16″N, −52°41′44.52″W), filtered and stored in a refrigerator.

Instrumentation

NMR spectra were recorded at room temperature using a Bruker Avance III 300 MHz spectrometer. Infrared spectra were recorded using a Bruker INVENIO-R Fourier Transform-Infrared Spectrometer (FT-IR), equipped with a diamond attenuated total reflectance (ATR) crystal. SEM micrographs were obtained on an FEI MLA 650F with samples coated in gold prior to imaging and carbon for EDX analysis. Reactions involving elevated pressures of CO_2 were carried out in a 300 mL Parr Instrument Company pressure vessel fitted with an internal temperature probe. The ultrasound used was from Misonix Ultrasonic Liquid Processors, paired with a Fisher Scientific Isotemp 30135 chiller to maintain isothermal conditions for the reaction over extended periods of time.

GC-MS was performed using an Agilent Technologies 7890A GC System, equipped with a DB-5MS column with the following parameters: length 30 m, diameter 0.180 mm, film 0.18 μm. The oven temperature was ramped from 150–300 °C, with a ramp rate of 10 °C min^{-1} and the inlet temperature set to 250 °C. The column flow was 1.1 mL min^{-1} using helium as the carrier gas. The MS source was set to 230 °C, with an MS Quad temperature of 150 °C. The column was run with a 3 min solvent delay and a 3 min hold.

DMA measurements were performed on a TA Discovery DMA 850. The strain ramp was measured using a fiber-film clamp with the following parameters: soak

10 min, temperature 30 °C, ramp rate 0.1 mm min^{-1}. All samples were run in duplicates at 30 °C under nitrogen.

Enzyme degradation studies

A pH 7 phosphate buffered solution (10.00 mL), containing 0.8 mol L^{-1} potassium chloride (KCl) was used for the studies. The solution was put in a 20 mL glass scintillation vial to which the 5.0 × 5.0 mm square of FO-NIPU was added. After equilibrating for 3 days, 50 μL of a lipase Novozym® 51032 was added. The vial was covered to reduce the light entering the solution.

Microbiology and molecular biology

BD Yeast Mold Broth, Lab-Grade Agar Powder, and Nuclease-free Water were purchased from VWR. The primers ITS1F (5′–3′ CTT GGT CAT TTA GAG GAA GTA A), ITS4 (5′–3′ TCC TCC GCT TAT TGA TAT GC), 16S rRNA Forward (5′–3′ AGA GTT TGA TCC TGG CTC AG), and 16S rRNA Reverse (5′–3′ ACG GCT ACC TTG TTA CGA CTT) were purchased from Integrated DNA Technologies. Promega GoTaq G2 Green Master Mix, 0.5 mm glass beads, 10X TBE Buffer (Tris–borate–EDTA), and 50X TAE Buffer (Tris–acetate–EDTA) were purchased from Thermo Scientific. Ethidium bromide solution (10 mg mL^{-1}) and certified molecular biology agarose powder were purchased from Bio-Rad. The method used to identify the mycelium and microbial populations of the samples was as previously described.[30]

Characterization of algae oil

Algae oil is a viscous pale yellow-green liquid with a grass-like odour. It was found to be soluble in common organic solvents. Its spectroscopic characterization is reported here. ^{1}H (300 MHz, CDCl$_3$): δ 0.88 (t, 5H, CH_3, J = 6.7 Hz), δ 0.97 (t, 3H, CH_3, J = 7.5 Hz), δ 1.26 (s, 30H, CH_2), δ 1.61 (m, 3H, CH_2), δ 2.07 (m, 4H, =CH–CH_2), δ 2.31 (t, 3H, O=C–CH_2, J = 7.5 Hz), δ 2.38 (m, 4H, O=C–CH_2), δ 2.83 (m, 11H, =CH–CH_2–CH=), δ 4.15 (m, 2H, O–CH_2–CHO–CH_2–O), δ 4.29 (d, 1H, O–CH_2–CHO–CH$_2$–O, J = 4.31 Hz), δ 4.33 (d, 1H, O–CH$_2$–CHO–CH_2–O, J = 4.4 Hz), and δ 5.38 (m, 15H, =CH–). ^{13}C NMR (75.0 MHz, CDCl$_3$): δ 14.12 (–CH$_3$), δ 14.27 (–CH$_3$), δ 20.57 (–CH$_2$–), δ 22.70 (–CH$_2$–), δ 24.87 (–CH$_2$–), δ 25.65 (–CH$_2$–), δ 29.67 (–CH$_2$–), δ 29.71 (–CH$_2$–), δ 31.93 (–CH$_2$–), δ 34.04 (–CH$_2$–), δ 62.03 (O–CH$_2$–CHO–CH$_2$–O), δ 69.08 (O–CH$_2$–CHO–CH$_2$–O), δ 127.03 (–CH=), δ 128.09 (–CH=), δ 128.58 (–CH=), δ 132.04 (–CH=), δ 172.14 (C=O), δ 172.53 (C=O), δ 173.27 (C=O). FT-IR (ATR, cm^{-1}): 3013 (w), 2922.89 (m), 2853 (m), 1743 (s), 1146 (w), 1098 (m).

Synthesis of fatty acid methyl esters (FAMEs)

Fatty acid methyl esters of the algae oil were prepared by the previously reported procedure. The molar mass of the triglyceride was approximated at 878 g mol^{-1}.[42] Algae oil (50.0 g) and methanol (13.8 mL) were combined in a 1 : 6 mol ratio with 0.5 wt% KOH (250 mg) and stirred until homogeneous. Ultrasonication was used to emulsify the mixture. With the amplitude of the ultrasound set to 75, power fluctuated between 65–71 W and ran for 20 min. The mixture was dissolved in 40 mL of diethyl ether and washed with an equivalent volume of water (3 × 65 mL). The sample was dried using anhydrous MgSO$_4$. Following filtration all

volatiles were removed under vacuum resulting in a pale-yellow oil (yield 82%). ^{1}H (300 MHz, CDCl$_3$): δ 0.88 (t, 5H, CH_3, J = 6.7 Hz), δ 0.97 (t, 3H, CH_3, J = 7.5 Hz), δ 1.26 (s, 30H, CH_2), δ 1.61 (m, 3H, CH_2), δ 2.07 (m, 4H, =CH–CH_2), δ 2.31 (t, 3H, O=C–CH_2, J = 7.5 Hz), δ 2.38 (m, 4H, O=C–CH_2), δ 2.83 (m, 11H, =CH–CH_2–CH=), δ 3.66 (s, 2H, CH_3–O–CO–), δ 3.67 (s, 2H, CH_3–O–CO–), δ 5.38 (m, 15H, =CH–). ^{13}C NMR (75.0 MHz, CDCl$_3$): δ 14.12 (–CH$_3$), δ 14.27 (–CH$_3$), δ 20.57 (–CH$_2$–), δ 22.70 (–CH$_2$–), δ 24.87 (–CH$_2$–), δ 25.65 (–CH$_2$–), δ 29.67 (–CH$_2$–), δ 29.71 (–CH$_2$–), δ 31.93 (–CH$_2$–), δ 34.04 (–CH$_2$–), δ 51.42 (CH$_3$O–C=O), δ 51.55 (CH$_3$O–C=O), δ 127.03 (–CH=), δ 128.09 (–CH=), δ 128.58 (–CH=), δ 132.04 (–CH=), δ 172.14 (C=O), δ 172.53 (C=O), δ 173.27 (C=O). FT-IR (ATR, cm^{-1}): 3013 (w), 2922.89 (m), 2853 (m), 1743 (s), 1436 (m), 1146 (w), 1098 (m).

Synthesis of epoxidized FAME (EFAME)

In a 100 mL round bottom flask, FAME (1.87 g) was dissolved in 40 mL of CH$_2$Cl$_2$ and m-CPBA (2.22 g) was slowly added. The flask was stoppered and stirred for 16 h. The mixture was washed with aqueous 1 M Na$_2$SO$_3$ (3 × 20 mL), followed by 1 M NaHCO$_3$ (3 × 20 mL), and 3 wt% NaCl (15 mL) solutions. The organic phase was dried using anhydrous MgSO$_4$, filtration and removal of solvents under vacuum yielding clear, colourless oils (yield 72%), which were kept refrigerated at 3 °C until required. ^{1}H (300 MHz, CDCl$_3$): δ 0.88 (t, 5H, CH_3, J = 6.7 Hz), δ 0.97 (t, 3H, CH_3, J = 7.5 Hz), δ 1.26 (s, 30H, CH_2), δ 1.61–1.80 (m, CH_2), δ 2.25–2.50 (m, =CH–CH_2), δ 2.31–3.25 (m, O=C–CH_2), δ 3.66 (s, 3H, CH_3–O–CO–), δ 3.67 (s, 3H, CH_3–O–CO–), δ 5.50 and 5.70 (m, $cyclo$-CH(O)CH). ^{13}C NMR (75.0 MHz, CDCl$_3$): δ 14.12 (–CH$_3$), δ 14.27 (–CH$_3$), δ 20.57 (–CH$_2$–), δ 22.70 (–CH$_2$–), δ 24.87 (–CH$_2$–), δ 25.65 (–CH$_2$–), δ 29.67 (–CH$_2$–), δ 29.71 (–CH$_2$–), δ 31.93 (–CH$_2$–), δ 34.04 (–CH$_2$–), δ 51.42 (CH$_3$O–C=O), δ 51.55 (CH$_3$O–C=O), δ 172.14 (C=O), δ 172.53 (C=O), δ 173.27 (C=O). FT-IR (ATR, cm^{-1}): 3012 (sh), 2916 (m), 2850 (m), 1749 (s), 1456 (w), 1378 (m), 1164 (m).

Synthesis of FAME cyclic carbonate (CFAME)

EFAME (400 mg) was combined with 11 mg of TBAB, and 3.0 mg of ascorbic acid in a 5 mL vial equipped with a small magnetic stir bar. The vials were placed inside a stainless-steel pressure vessel. The vessel was placed in an oil bath on a hotplate-stirrer, pressurized to 10 bar CO$_2$ and heated to an internal temperature of 110 °C. The reaction proceeded for 48 h before cooling and venting of CO$_2$ resulting in the formation of brown liquid products. Using this method reactions could be scaled up to use 1.00 g of epoxide, 55 mg of TBAB and 15 mg of ascorbic acid. Yield 60–78%. ^{1}H (300 MHz, CDCl$_3$): δ 0.88 (t, 5H, CH_3, J = 6.7 Hz), δ 0.97 (t, 3H, CH_3, J = 7.5 Hz), δ 1.26 (s, 30H, CH_2), δ 1.61 (m, 3H, CH_2), δ 2.07 (m, 4H, CH_2), δ 2.31 (t, 3H, O=C–CH_2, J = 7.5 Hz), δ 2.38 (m, 4H, O=C–CH_2), δ 2.83 (m, 11H, OCH–CH_2–CHO), δ 3.66 (s, 2H, CH_3–O–CO–), δ 3.67 (s, 2H, CH_3–O–CO–), δ 4.2–4.9 (m, cyclic carbonate). ^{13}C NMR (75.0 MHz, CDCl$_3$): δ 14.12 (–CH$_3$), δ 14.27 (–CH$_3$), δ 20.57 (–CH$_2$–), δ 22.70 (–CH$_2$–), δ 24.87 (–CH$_2$–), δ 25.65 (–CH$_2$–), δ 29.67 (–CH$_2$–), δ 29.71 (–CH$_2$–), δ 31.93 (–CH$_2$–), δ 34.04 (–CH$_2$–), δ 51.42 (CH$_3$O–CHO), δ 51.55 (CH$_3$O–CHO), δ 172.14 (C=O), δ 172.53 (C=O), δ 173.27 (C=O). FT-IR (ATR, cm^{-1}): 3012 (sh), 2923 (m), 2853 (m), 1791 (s), 1736 (m) 1459 (m), 1365 (m), 1170 (m), 1047 (m).

Synthesis of NIPU

100 mg of the carbonated FAME was combined with 200 mg of Cardolite™ NC-540. The mixture was heated to 40 °C then transferred to a 100 °C oven for 24 h. The resulting red film was characterized by infrared spectroscopy. The FT-IR (ATR, cm^{-1}) spectrum observed was similar to that of the carbonated FAME with appearance of bands at 3298 cm^{-1} and 1736 cm^{-1}, and disappearance of bands at 1740 cm^{-1} and 1791 cm^{-1}. DMA parameters for samples run in duplicate are shown in Table 3.

Data availability

Data supporting this article have been included as part of the ESI.†

Author contributions

C. M. K. and F. M. K. conceived the work and supervised the project. J. E. P., C. M. L. and M. D. W. performed the experimental work, data analysis and drafted material for the manuscript. M. M. F. performed the DMA analysis and interpretation.

Conflicts of interest

There are no conflicts to declare.

Acknowledgements

References

1 A. Bruckbauer, G. B. Scofield, T. Frisch, M. W. Halloran, Z. C. Guan, K. M. J. Wnuk-Fink, M. N. Allemann, K. O'Shea, R. Simkovsky, J. Bae, S. P. Mayfield and M. D. Burkart, *Chem. Mater.*, 2025, **37**, 1561–1569.

2 M. MacLeod, H. P. H. Arp, M. B. Tekman and A. Jahnke, *Science*, 2021, **373**, 61–65.

3 H. Sardon, D. Mecerreyes, A. Basterretxea, L. Avérous and C. Jehanno, *ACS Sustainable Chem. Eng.*, 2021, **9**, 10664–10677.

4 Y. Q. Zhu, C. Romain and C. K. Williams, *Nature*, 2016, **540**, 354–362.

5 L. Filiciotto and G. Rothenberg, *ChemSusChem*, 2021, **14**, 56–72.

6 H. Blattmann, M. Fleischer, M. Bähr and R. Mülhaupt, *Macromol. Rapid Commun.*, 2014, **35**, 1238–1254.

7 A. Cornille, R. Auvergne, O. Figovsky, B. Boutevin and S. Caillol, *Eur. Polym. J.*, 2017, **87**, 535–552.

8 A. Gomez-Lopez, S. Panchireddy, B. Grignard, I. Calvo, C. Jerome, C. Detrembleur and H. Sardon, *ACS Sustainable Chem. Eng.*, 2021, **9**, 9541–9562.

9 M. S. Kathalewar, P. B. Joshi, A. S. Sabnis and V. C. Malshe, *RSC Adv.*, 2013, **3**, 4110–4129.

10 L. Maisonneuve, O. Lamarzelle, E. Rix, E. Grau and H. Cramail, *Chem. Rev.*, 2015, **115**, 12407–12439.

11 S. Doley and S. K. Dolui, *Eur. Polym. J.*, 2018, **102**, 161–168.

12 M. Y. Yao, Y. B. Huang, X. Niu and H. Pan, *ACS Sustainable Chem. Eng.*, 2016, **4**, 3840–3849.

13 S. Samanta, S. Selvakumar, J. Bahr, D. S. Wickramaratne, M. Sibi and B. J. Chisholm, *ACS Sustainable Chem. Eng.*, 2016, **4**, 6551–6561.

14 M. Bähr and R. Mülhaupt, *Green Chem.*, 2012, **14**, 483–489.

15 I. Javni, D. P. Hong and Z. S. Petrovic, *J. Appl. Polym. Sci.*, 2008, **108**, 3867–3875.

16 T. Dong, E. P. Knoshaug, R. Davis, L. M. L. Laurens, S. Van Wychen, P. T. Pienkos and N. Nagle, *Algal Res.*, 2016, **19**, 316–323.

17 P. T. Pienkos and A. Darzins, *Biofuels, Bioprod. Biorefin.*, 2009, **3**, 431–440.

18 T. Dong, E. P. Knoshaug, P. T. Pienkos and L. M. L. Laurens, *Appl. Energy*, 2016, **177**, 879–895.

19 T. Dong, E. Dheressa, M. Wiatrowski, A. P. Pereira, A. Zeller, L. M. L. Laurens and P. T. Pienkos, *ACS Sustainable Chem. Eng.*, 2021, **9**, 12858–12869.

20 Cardolite NC-540 is a phenalkamine that can be used as an amine-based epoxy curing agent. It is a mixture of *meta*-C15-alkenylphenols with varying degrees of unsaturation, including 3-(penta-dec-8-en-1-yl)-, 3-(pentadeca-8,11-dien-1-yl)-, and 3-(pentadeca-8,11,14-trien-1-yl)phenols.

21 C. M. Laprise, K. A. Hawboldt, F. M. Kerton and C. M. Kozak, *Macromol. Rapid Commun.*, 2021, **42**, 2000339.

22 I. A. Adeoti and K. Hawboldt, *Fuel*, 2015, **158**, 183–190.

23 P. Roesle, F. Stempfle, S. K. Hess, J. Zimmerer, C. Rio Bartulos, B. Lepetit, A. Eckert, P. G. Kroth and S. Mecking, *Angew. Chem., Int. Ed.*, 2014, **53**, 6800–6804.

24 S. Chikkali and S. Mecking, *Angew. Chem., Int. Ed.*, 2012, **51**, 5802–5808.

25 U. Biermann, U. Bornscheuer, M. A. R. Meier, J. O. Metzger and H. J. Schäfer, *Angew. Chem., Int. Ed.*, 2011, **50**, 3854–3871.

26 R. Goss and C. Wilhelm, Lipids in Algae, Lichens and Mosses, in *Lipids in Photosynthesis: Essential and Regulatory Functions*, ed. H. Wada and N. Murata, 2009, vol. 30, pp. 117–137.

27 G. B. Cai, S. F. Chen, L. Liu, J. Jiang, H. B. Yao, A. W. Xu and S. H. Yu, *CrystEngComm*, 2010, **12**, 234–241.

28 G. X. De Hoe, M. T. Zumstein, B. J. Tiegs, J. P. Brutman, K. McNeill, M. Sander, G. W. Coates and M. A. Hillmyer, *J. Am. Chem. Soc.*, 2018, **140**, 963–973.

29 G. L. Gregory, G. S. Sulley, L. P. Carrodeguas, T. T. D. Chen, A. Santmarti, N. J. Terrill, K. Y. Lee and C. K. Williams, *Chem. Sci.*, 2020, **11**, 6567–6581.

30 J. L. Vidal, B. M. Yavitt, M. D. Wheeler, J. L. Kolwich, L. N. Donovan, C. S. Sit, S. G. Hatzikiriakos, N. K. Jalsa, S. L. MacQuarrie and F. M. Kerton, *Sustainable Chem. Pharm.*, 2022, **25**, 100586.

31 G. Webster, A. J. Mullins, A. S. Bettridge, C. Jones, E. Cunningham-Oakes, T. R. Connor, J. Parkhill and E. Mahenthiralingam, *Microbiol. Resour. Announce.*, 2019, **8**, e0077819.

32 R. C. Wilhelm, S. J. L. Murphy, N. M. Feriancek, D. C. Karasz, C. M. DeRito, J. D. Newman and D. H. Buckley, *Int. J. Syst. Evol. Microbiol.*, 2020, **70**, 2137–2146.

33 M. Rahman, A. A. Sabir, J. A. Mukta, M. M. A. Khan, M. Mohi-Ud-Din, M. G. Miah, M. Rahman and M. T. Islam, *Sci. Rep.*, 2018, **8**, 2504.

34 E. Estévez, M. C. Veiga and C. Kennes, *Appl. Microbiol. Biotechnol.*, 2005, **67**, 563–568.

35 D. Zhao, B. Liu, L. Y. Li, X. F. Zhu, Y. Y. Wang, J. Q. Wang, Y. X. Duan and L. J. Chen, *Biocontrol Sci. Technol.*, 2013, **23**, 980–986.

36 C. Ratledge, H. Streekstra, Z. Cohen and J. Fichtali, Downstream Processing, Extraction, and Purification of Single Cell Oils, in *Single Cell Oils*, ed. Z. Cohen and C. Ratledge, AOCS Press, 2nd edn, 2010, pp. 179–197.

37 M. Tariq, A. K. Qureshi, S. Karim, M. Sirajuddin, N. Abbas, M. Imran and J. H. Shirazi, *Energy*, 2021, **222**, 120014.

38 Z. S. Petrovic, X. M. Wan, O. Bilic, A. Zlatanic, J. Hong, I. Javni, M. Ionescu, J. Milic and D. Degruson, *J. Am. Oil Chem. Soc.*, 2013, **90**, 1073–1078.

39 K. M. Doll and S. Z. Erhan, *J. Agric. Food Chem.*, 2005, **53**, 9608–9614.

40 L. Poussard, J. Mariage, B. Grignard, C. Detrembleur, C. Jérôme, C. Calberg, B. Heinrichs, J. De Winter, P. Gerbaux, J. M. Raquez, L. Bonnaud and P. Dubois, *Macromolecules*, 2016, **49**, 2162–2171.

41 A. R. Mahendran, N. Aust, G. Wuzella, U. Müller and A. Kandelbauer, *J. Polym. Environ.*, 2012, **20**, 926–931.

42 C. Stavarache, M. Vinatoru, R. Nishimura and Y. Maeda, *Ultrason. Sonochem.*, 2005, **12**, 367–372.